Published online October 3, 2006

Using Soil Freezing Characteristics to Model Multi-Season Soil Water Dynamics

G. N. Flerchinger,* M. S. Seyfried, and S. P. Hardegree

ABSTRACT

The soil moisture characteristic (SMC) is a fundamental soil property for simulating soil water dynamics but is difficult and time-consuming to measure. When the soil is frozen, the soil water potential and liquid water content are strongly dependent on temperature. The relation between soil freezing temperatures and liquid water content, termed the *soil freezing characteristic* (SFC), is related to the SMC. With the widespread use of time-domain reflectometry (TDR) to measure liquid water in frozen soil, simultaneous measurement of soil temperature and liquid water content under frozen conditions enables in situ estimation of the SMC curve through its similarity to the SFC. We investigated the applicability of deducing the SMC curve from in situ measurements of the SFC for simulation of both frozen and unfrozen soil water dynamics. Results suggest that SMC parameters deduced from the SFC may be used for model simulations without a significant loss of accuracy, as compared with model simulations based on pressure plate analyses.

Liquid water in the soil exists in equilibrium with ice at temperatures well below the normal freezing point of water (0°C). When ice is present in the soil, the soil water potential and liquid water content are strongly influenced by temperature. As soil temperature drops further below the soil water freezing point, water potential becomes more negative, more water freezes, and liquid water content decreases. This drop in liquid water content and water potential during freezing is analogous to soil drying. The relation between freezing soil temperatures and liquid water content is referred to as the soil freezing characteristic (SFC) and is similar to the soil moisture characteristic (SMC) for unfrozen soil (Koopmans and Miller, 1966; Spaans and Baker, 1996; Bittelli et al., 2003).

Measurement of the SMC is time-consuming, particularly for water potentials less than -500 J kg^{-1} because of the long equilibration time required. In arid and semiarid regions, matric potentials much lower than this are common due to surface evaporation and the low extraction limits (less than -4000 J kg^{-1}) of adapted vegetation (Seyfried et al., 2005). Spaans and Baker (1996) demonstrated the direct correspondence between the SFC and the SMC and the advantages of using the SFC to determine water retention properties at low matric potentials. In many northern latitudes, in situ soil temperature can often be measured down to -8°C, enabling estimation of the SMC down to a corresponding water potential of approximately $-10\,000$ J kg^{-1}. Bittelli et al. (2003) took advantage of the similarity between the SFC and SMC to rapidly measure water retention characteristics in the laboratory. These curves were limited to thawing processes (analogous to wetting processes) as supercooling phenomenon is common during freezing in laboratory settings.

Widespread use of TDR to measure liquid water in frozen soil enables in situ estimation of the SFC through simultaneous measurement of soil temperature and liquid water content when the soil is frozen and ice is present in the soil pores. The relation between the SFC and SMC enables estimation of the SMC curve from these in situ measurements. We investigated the applicability of SMC curves obtained from in situ measurement of the SFC for simulating both frozen and unfrozen soil water dynamics.

THEORY

When ice is present, soil water potential is a function of temperature and can be expressed by the generalized form of the Clapeyron equation:

$$d\phi = (L_f/T)dT + d\phi_i \quad [1]$$

where ϕ is the equilibrium total water potential (J kg^{-1}), ϕ_i is the ice potential (J kg^{-1}), L_f is latent heat of fusion (J kg^{-1}), and T is absolute temperature (K). Spaans and Baker (1996) presented an integrated form of the Clapeyron equation for computing total water potential (kJ kg^{-1}) incorporating the temperature dependency of the latent heat of fusion and assuming zero gauge pressure in ice:

$$\phi = \psi + \pi = -712.38\ln(T/T_0) + 5.545(T - T_0) - 3.14 \times 10^{-3}(T^2 - T_0^2) \quad [2]$$

Here ψ is soil matric potential (kJ kg^{-1}), π is soil water osmotic potential (kJ kg^{-1}), and T_0 is a reference temperature (273.15 K). Thus, when ice is present in the soil, heat and water flux through the soil are tightly coupled. That is, the matric potential, and therefore liquid water content, are defined by the temperature and osmotic potential. This assumes that the soil is wet enough for the soil water to freeze at the temperatures experienced. If the soil is sufficiently dry or contains ample solutes such that the soil water is below the equilibrium water potential given by Eq. [2], soil water will not freeze. Without ice present, the relation between temperature and soil water potential does not apply.

G.N. Flerchinger, M.S. Seyfried, and S.P. Hardegree, USDA-ARS, Northwest Watershed Research Center, Boise, ID 83712. Received 27 May 2005. *Corresponding author (gflerchi@nwrc.ars.usda.gov).

Published in Vadose Zone Journal 5:1143–1153 (2006).
Original Research
doi:10.2136/vzj2006.0025

677 S. Segoe Rd., Madison, WI 53711 USA

Abbreviations: MBE, mean bias error; ME, model efficiency; RMSD, root mean square deviation; SFC, soil freezing characteristic; SHAW, Simultaneous Heat and Water [model]; SMC, soil moisture characteristic; TDR, time-domain reflectometry; WCR, water content reflectometer.

A variety of expressions are used to describe the SMC curve. The expression used in this study is (Campbell, 1974)

$$\psi = \psi_e \left(\frac{\theta_l}{\theta_s}\right)^{-b} \quad [3]$$

where ψ_e is air entry potential (J kg^{-1}), b is a pore size distribution parameter, θ_l is liquid water content (m^3 m^{-3}), and θ_s is saturated water content (m^3 m^{-3}). Water flux equations and the relation between matric potential and liquid water content defined by the SMC is typically assumed valid for frozen conditions (Koopmans and Miller, 1966; Fuchs et al., 1978).

For most soils, the influence of osmotic potential on the SFC is a rather small component of the total water potential, particularly at low matric potentials. However, for accurate determination of the SMC near saturation, the osmotic potential (kJ kg^{-1}) should be taken into consideration, particularly for soils high in solutes. This can be done by measuring the electrical conductivity of a saturated paste extract and estimating osmotic potential by (Spaans and Baker, 1996)

$$\pi = 39\sigma_{sp}\left(\frac{w_{sp}\rho_b}{\theta\rho_l^2}\right)(T/T_{sp}) \quad [4]$$

where σ_{sp} is electrical conductivity of a saturated paste extract (mS cm^{-1}), w_{sp} is gravimetric water content of the soil sample for the saturated extract (typically 0.5 kg kg^{-1}), ρ_b is bulk density (kg m^{-3}), ρ_l is density of water, and T_{sp} is the temperature (K) at which σ_{sp} was measured.

MATERIALS AND METHODS

In this study, correspondence between in situ SFCs and SMCs measured in the laboratory was demonstrated using three soil types at the Orchard Field Test Site in southwest Idaho where measured SMCs were obtained. Model simulations using laboratory-measured SMCs were compared with simulations using the SFC to estimate the SMC. Applicability of the SFC measured in situ to estimate the SMC for simulation of soil water dynamics was further investigated on rangeland sites on the Boise Front and in the Reynolds Creek Experimental Watershed. Existing field installations having moderately accurate soil temperature sensors (nominal field accuracy ± 0.15 C) were used rather than installing more accurate sensors typically not used in the field.

The Simultaneous Heat and Water (SHAW) model (Flerchinger and Saxton, 1989; Flerchinger and Pierson, 1991) was used to simulate the soil water dynamics for all sites. Simulated daily liquid water contents were compared with measured values using performance measures summarized in Table 1. Model efficiency (ME) is analogous to the coefficient of determination, with the exception that ME ranges from negative infinity to 1.0; negative ME values indicate that the mean observation is a better predictor than simulated values. Root mean square deviation (RMSD) is a measure of the absolute difference between simulated and measured values, while mean bias error (MBE) is an indicator of the bias in simulated values compared to observations.

Orchard Site

The Orchard site (43°19′ N, 115°59′ W) was described in detail by Flerchinger and Hardegree (2004) who used the SHAW model to simulate near-surface soil temperature and water conditions for the 1995 spring germination season. The site is flat and receives approximately 293 mm of precipitation annually. Three microclimatic monitoring sites were established within 400 m of each other, one in each of three soil types: loamy sand, sandy loam, and silt loam, determined by hydrometer method (Gee and Bauder, 1986). Each monitoring site consisted of six plots, three maintained for bare soil and three maintained for annual cheatgrass (*Bromus tectorum* L.) cover. This study focuses on the bare soil plots during the 1997–1998 winter.

Table 1. Description and definition of model performance measures.

Measure	Description	Mathematical definition†
ME	Model Efficiency, i.e., variation in measured values accounted for by the model.	$1-\frac{\sum_{i=1}^{N}(Y_i-\hat{Y}_i)^2}{\sum_{i=1}^{N}(Y_i-\overline{Y})^2}$
RMSD	Root Mean Square Difference between simulated and observed values.	$\left[\frac{1}{N}\sum_{i=1}^{N}(\hat{Y}_i-Y_i)^2\right]^{1/2}$
MBE	Mean Bias Error of model predictions compared to observed values.	$\frac{1}{N}\sum_{i=1}^{N}(\hat{Y}_i-Y_i)$

† $\hat{Y}_i$ = simulated values; Y_i = observed values; $\overline{Y}$ = mean of observed values; N = number of observations.

Detailed descriptions of instrumentation and soil sampling are given by Flerchinger and Hardegree (2004). Thermocouples recorded hourly soil temperature at depths of 1, 2, 5, 10, 20, 30, 50, and 100 cm in each plot. Three-prong 20-cm TDR waveguides were read hourly at these same depths, except for the 1-cm depth. The soil apparent relative permittivity (ξ_a) was determined from electronic pulse travel time with a Trase TDR (Soilmoisture Equipment Inc., Santa Barbara, CA) and converted to water content using the manufacturer-supplied calibration, which closely approximates to the Topp et al. (1980) equation.

Ice in the soil can influence liquid content readings from TDR-based measurements. Although the influence is usually small, it is a consistent bias in the reading. Spaans and Baker (1995) proposed calibration of TDR for liquid water based on total water content, which requires developing a family of curves for varying total water content. This can be difficult to obtain and requires knowledge of the total water content. Without accurate knowledge of the total water content, we took a more simple approach to correcting for ice content. The apparent bulk complex permittivity (ξ_a) measured by TDR can be approximated by

$$\xi_a^n = \theta_l\xi_l^n + \theta_m\xi_m^n + \theta_g\xi_g^n + \theta_i\xi_i^n \quad [5]$$

where θ_l, θ_m, θ_g, and θ_i are the volumetric liquid water, mineral, gas, and ice contents of the soil; ξ_l, ξ_m, ξ_g, and ξ_i are the respective dielectric constants; and n is an empirical exponent (Seyfried and Murdock, 1996; Bittelli et al., 2004). An equation of the form

$$\theta_w = a + b\xi_a^n \quad [6]$$

fitted to the θ_l–ξ_a look-up table provided by the Trase manual (Soilmoisture, 1990) yielded a value of 0.53 for n ($R^2 = 0.994$). Using Eq. [6], ξ_a was back-calculated from the water content provided by the Trase TDR, then a corrected water content was calculated using Eq. [5] with assumed values of 90, 5.0, 1.0, and 3.3 for ξ_w, ξ_m, ξ_g, and ξ_i. (While values of 90 and 5.0 are very realistic for ξ_w and ξ_m near 0°C, these values can be computed

from the best-fit coefficients in Eq. [6] using an assumed porosity of 0.55 in Eq. [5].) Total water content was estimated by interpolating between water content readings before and after the freeze–thaw cycle, unless the thaw coincided with snowmelt or rainfall, in which case total water content at the beginning of the freeze–thaw cycle was used.

Meteorologic stations at each of the three sites collected air temperature, precipitation, wind speed, humidity, and solar radiation. Soil textural analysis and density samples were taken at 10-cm intervals to a depth of 100 cm in addition to a 5-cm sample. Sites A and B are classified within the Tindahay series (sandy, mixed, mesic Xeric Torriorthents). Site A is a Tindahay loamy sand, and Site B is a Tindahay sandy loam. Site C is classified as a Lankbush silt loam (fine-loamy, mixed, superactive, mesic Xeric Haplargids).

Pressure plate measurements were conducted on soil surface (<20 cm) samples collected from each of the three sites to determine the SMC. Soil samples were compacted into 65-mm diameter by 50-mm rings for pressure plate analysis. Water content measurements were taken at 11 water potential settings ranging from −10 to −1500 J kg^{-1}. Soil moisture characteristic parameters given in Table 2 were obtained by a nonlinear least-squares fit to the pressure plate data. Electrical conductivity readings of saturated paste extracts (Rhoades, 1986) were taken from surface 10-cm soil samples (Table 2).

Lower Sheep Creek

The Lower Sheep Creek site is a subwatershed within the Reynolds Creek Experimental Watershed in southwest Idaho. The site is located at an elevation of 1620 m and receives 361 mm of average annual precipitation. The area has sparse sagebrush cover with essentially bare ground in the interspace areas between plants. The soil is classified as fine-loamy, montmorillonitic, frigid Typic Argixeroll. The site has a west-facing slope of 17%. Near-surface (top 20 cm) hydraulic conductivity measured with a Guelph permeameter was found to be approximately 2.7 cm h^{-1}.

Hourly weather observations of air temperature, wind speed, humidity, and solar radiation were collected at the site along with break point precipitation data. Instrumentation was installed to measure soil water and temperature profiles to a depth of 1 m at four locations, two located under sagebrush plants and two located in the bare interspace area. Hourly soil temperatures were measured near the surface (within the top 5 cm) and at depths of 10, 20, 40 65 and 100 cm using YSI two-thermistor composite thermolinear components (Yellow Springs Instruments, Yellow Springs, OH) accurate to ±0.15°C between −30 and 50°C. Soil water was measured hourly using fiberglass resistance sensors calibrated with approximately weekly readings of liquid water content using TDR as described by Seyfried (1993). No correction for ice content was performed for the liquid water content measurements from the fiberglass resistance sensors because the sensors were calibrated to TDR using predominantly data during unfrozen periods; the presence of ice is expected to have a minimal effect on the fiberglass sensor readings (electrical conductivity of ice can be taken as zero), and no methodology has been developed to correct for any influence. Seyfried (1993) demonstrated that the fiberglass sensors work well under frozen and unfrozen conditions.

Table 2. Moisture characteristic curve parameters† for each of the sites as determined from the soil freezing characteristic (SFC). Pressure plate analyses were available for only the Orchard sites.

Site	Saturated paste extract	θ_s	Pressure plate		SFC	
			b	ψ_e	b	ψ_e
	mS cm^{-1}	m^3 m^{-3}		J kg^{-1}		J kg^{-1}
Orchard Site A	0.126	0.39	3.16	−1.3	2.92	−1.6
Orchard Site B	0.162	0.46	3.24	−4.4	2.62	−1.6
Orchard Site C	0.438	0.55	3.51	−6.1	2.54	−8.3
Lower Sheep	n/a	0.50	n/a	n/a	4.75	−11.2
Boise Front	0.319	0.44	n/a	n/a	2.52	−7.2

† $\psi = \psi_e(\theta/\theta_s)^{-b}$.

Boise Front

Data from the Boise Front were collected at a site in the Dry Creek watershed near Boise, ID. Soil at the site is classified as coarse-loamy, mixed mesic, Pachic Ultic Haploxeroll. Soil texture, determined by hydrometer method, is loam from 0 to 100 cm. A standard meteorological station installed 30 m from the soil monitoring site measured air temperature, precipitation, wind speed, humidity, and solar radiation. Vegetation consisted of a mixture of grasses and forbs covering 63% of the surface as obtained by point-intercept method of two 10-m transects.

Two pits, separated by about 1.5 m, were excavated to a depth of 100 cm. In each pit, soil water content and temperature were measured with paired CS615 water content reflectometers (WCR) (Campbell Scientific, 1996) and thermocouples installed at depths of 5, 15, 30, 50, and 100 cm. The WCRs and thermocouples were sampled at 15-min intervals. The WCR is a transmission line oscillator that, like TDR, can determine ξ_a from the pulse travel time (Kelleners et al., 2005; Campbell and Anderson, 1998). Like TDR, water content obtained by WCRs corresponds to liquid water content in frozen soil (Bittelli et al., 2003). The ξ_a–θ_l relationship for the WCR may be different from that measured with TDR because the WCR measurement frequency is much lower than that of TDR (Seyfried and Murdock, 2001). For this reason, WCR data were calibrated using colocated TDR waveguides by Chandler et al. (2004), who obtained excellent calibrations of WCR-measured periods with TDR-measured ξ_a. Because the WCRs were calibrated to TDR and the period measured by the WCRs respond to ice content similar to the ξ_a of the TDR, the same procedure was used to correct for ice content as described for the Orchard sites.

SHAW Model Description

The SHAW model is a one-dimensional model originally developed to simulate soil freezing and thawing processes (Flerchinger and Saxton, 1989). Utility of the model has expanded and has been demonstrated for predicting climate and management effects on soil freezing (Xu et al., 1991; Hayhoe, 1994; Kennedy and Sharratt, 1998), snowmelt (Flerchinger et al., 1994, 1996a), soil temperature, soil water (Flerchinger and Pierson, 1991; Hymer et al., 2000; McDonald, 2002), evapotranspiration and water balance (Flerchinger et al., 1996b, 1998; Parkin et al., 1999).

The SHAW model simulates a vertical profile extending from the top of a plant canopy or the snow, residue, or soil surface to a specified depth within the soil. Weather conditions above the upper boundary and soil conditions at the lower boundary define heat and water fluxes into the system. Water and heat flux at the surface boundary include absorbed solar radiation, long-wave radiation exchange, and turbulent transfer of heat and vapor. Soil water flux is computed using an implicit solution to the mixed form of the Richards equation (Celia et al., 1990) with provisions for soil freezing.

COMPARISON OF SOIL FREEZING AND SOIL MOISTURE CHARACTERISTICS

Parameter Comparison

Hourly soil temperatures are plotted against corresponding measured water contents for all subzero temperatures (°C) during the fall–winter season of 1997–1998 for the Orchard Site C in Fig. 1a. Equilibrium matric potential computed from Eq. [2] and [4] based on freezing temperatures and water content are plotted against water content in Fig. 1b, producing a SFC for the soil. The points measured by pressure plate analysis plot nicely along the upper bound of the points representing the SFC.

A log-log plot of matric potential versus water content for all three sites presented in Fig. 2 begins to show some of the weaknesses of the SFC in deducing the SMC. Particularly for Sites A and C, the points are increasingly more scattered at high (less negative) matric potentials. Thus, there is considerable uncertainty in the SMC obtained from the SFC at high water contents. Two major issues contribute to this uncertainty: the influence of solutes and the accuracy of the temperature measurement are both more critical at the higher water contents, as will be discussed later.

Also plotted in Fig. 2 are the best-fit lines from the SFC. Coefficient of determinations (R^2) for Sites A, B, and C are 0.21, 0.48, and 0.41, respectively. Best-fit SMC

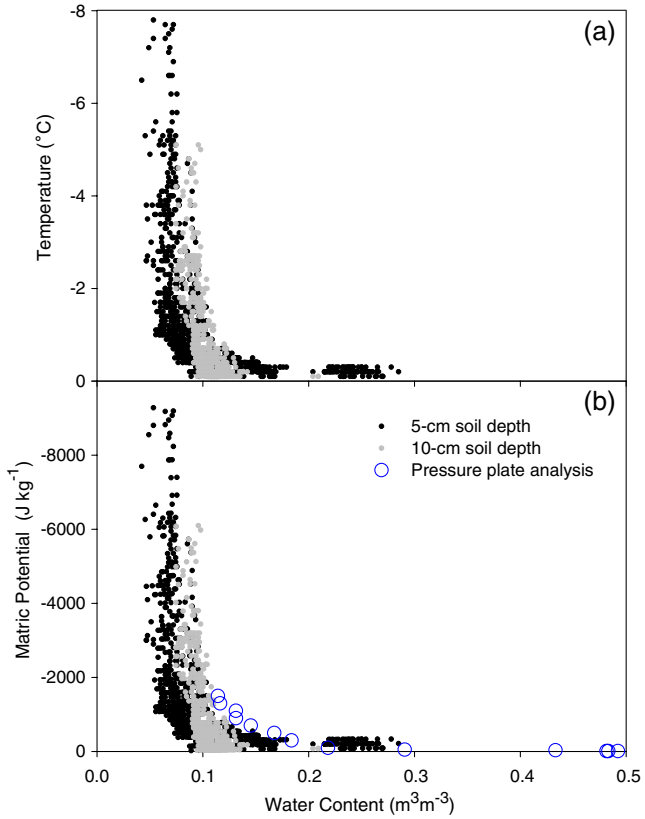

Fig. 1. (a) Freezing temperatures and (b) associated water potential versus liquid water content for the silt loam Orchard Field Site C. Points of soil moisture curve measured by pressure plate shown for comparison.

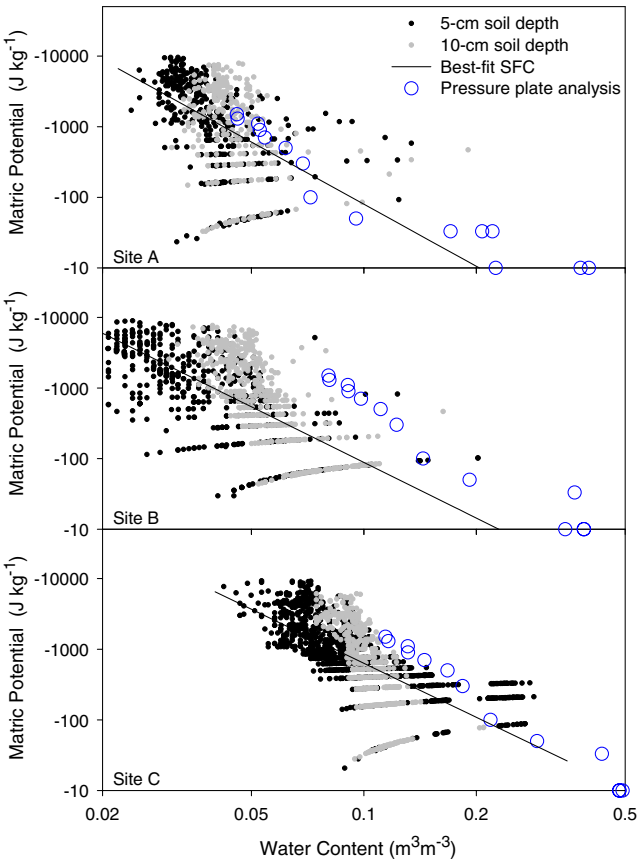

Fig. 2. Log-log plot of matric potential versus water content from the Orchard Field Site A (loamy sand), Site B (sandy loam), and Site C (silt loam). Plotted are the matric potential estimated from freezing temperatures for the 5- and 10-cm depths, the resulting best-fit curve for the soil freezing characteristic (SFC), and pressure plate measurements.

parameters obtained from the SFC and from pressure plate analysis are presented in Table 2. For Plots A and C, the best-fit line from the SFC roughly matches the points obtained from pressure plate analysis, but for Site B, there is a considerable offset, which translates to a discrepancy in ψ_e between the SFC and pressure plate parameters (Table 2). Indeed ψ_e determined by pressure plate analysis for Site B is outside the 90% confidence interval (-0.35 to -1.07 J kg^{-1}) of the SFC parameter estimate, as is the b value (2.46–2.77 confidence interval). The cause for this discrepancy is unclear. The b value from the pressure plate analysis of Site C is also outside the 90% confidence interval (2.40–2.69) for the SFC-based estimate. Coefficients from the pressure plate analysis for Site A are within the confidence intervals of the SFC parameter estimates. Given the rather poor R^2 for Site A, perhaps it is a bit fortuitous that the SFC parameter estimates agree so closely with the parameters from the pressure plate analysis.

Influence on Simulated Soil Water Dynamics

Model simulations using SMC parameters obtained from pressure plate analyses and the SFC were compared to assess the influence of the uncertainty in estimated parameters. Soil water dynamics were simulated

by the SHAW model from Day 309 (early November) of 1997 to Day 180 (late June) of 1998 for the three soils at the Orchard site using both sets of SMC parameters given in Table 2. Simulations were conducted to a depth of 4 m, where soil temperature was assumed constant and water flux was assumed to be by gravity flow only. The parameters obtained from pressure plate analyses are the same parameters used for the 1995 spring simulation reported by Flerchinger and Hardegree (2004). Calibrated values for saturated hydraulic conductivity reported by Flerchinger and Hardegree (2004) were used.

The SMC parameters obtained by the two methods were most disparate for the sandy loam Site B. Soil water dynamics during the freezing period are illustrated for Site B in Fig. 3. Frozen conditions can be observed from the water content plotted for the 5-, 10-, and 20-cm depths by separation of the simulated liquid water content line from the total water content line; the difference between the two lines is ice content. Model performance for simulating daily liquid water content during the freezing period is summarized in Table 3 and during the nonfreezing period in Table 4. Liquid water contents from the SFC-based simulation were consistently lower than the measurements and the pressure plate–based simulation during the freeze cycles between Day 345 of 1997 and Day 5 of 1998, but slightly higher than the pressure plate–based simulation subsequent to the freeze cycles. Interestingly, model performance measures for Site B are slightly better for the SFC-based simulation (Table 3), perhaps owing to the fact that the SFC was measured in situ.

The *F* tests given in Tables 3 and 4 comparing RMSD values for simulations using the different parameter sets show no significant differences. Because simulation errors are strongly autocorrelated, the number of independent samples is considerably less than the number of daily observations. Effective sample sizes reported in Tables 3 and 4 were computed from the expression given by Lee and Lund (2004) adjusting for the lag-one autocorrelation of the residual series; lag-one correlations ranged from 0.10 to 0.97 with the deeper depths typically having a higher lag correlation. Unfortunately this considerably reduced sample size and the power to distinguish differences. Neglecting the correction for autocorrelated errors, significant differences in RMSD were detected at the $p = 0.05$ level for the nonfreezing period at Site C (sample size equals 77). The lower *b* value for SFC-based parameters for Site C resulted in smaller matric potential gradients and less upward water migration for the SFC-based simulation. The lower simulated water contents of the SFC-based simulation for Site C actually improved the model performance during the freezing period where the pressure plate–based simulation tended to overpredict water contents (Table 3), but were a detriment during the nonfreezing period when water contents were already underpredicted.

Soil water dynamics for the coarsely textured Sites A and B were considerably less responsive to freeze–thaw processes than the silt loam Site C. Water contents for Site C are plotted in Fig. 4. Elevated total water content

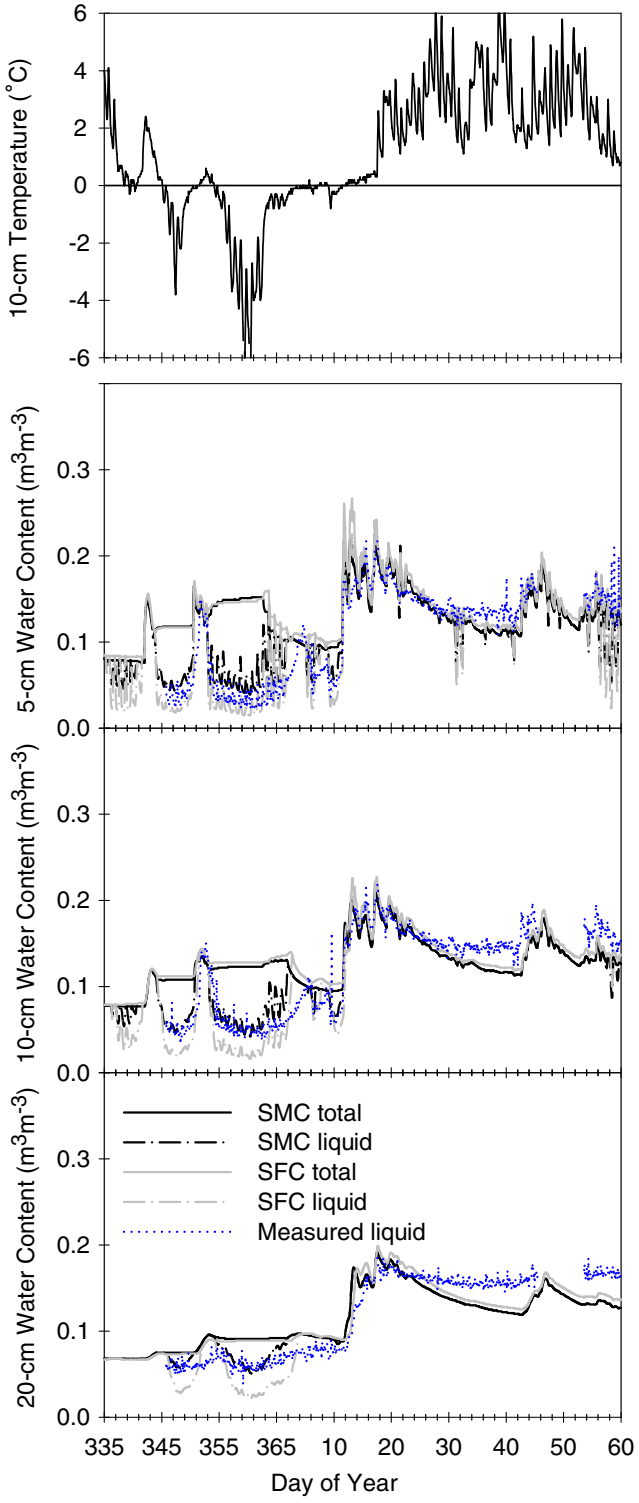

Fig. 3. Simulated hourly water contents using soil moisture characteristic (SMC) parameters estimated from the soil freezing characteristic (SFC) and from pressure plate analyses. Plotted are total water content and simulated and measured liquid water content for the sandy loam Orchard Field Site B for the 5-, 10-, and 20-cm depths. The 10-cm soil temperatures are plotted for reference to freeze–thaw cycles.

due to water migration to the freezing front can be observed for all three depths. As the 5-cm depth began to freeze on Day 344, total water content began to increase

Table 3. Model performance for simulated daily liquid water content at the Orchard sites during the freezing period (November through February) using parameters based on pressure plate analysis and estimated from the soil freezing characteristic (SFC).

	Pressure plate parameters			SFC parameters			
Depth	ME	RMSD	MBE	ME	RMSD	MBE	*F* test†
cm		$m^3\ m^{-3}$			$m^3\ m^{-3}$		
				Site A			
5	0.744	0.022	−0.017	0.640	0.027	−0.021	$p(27, 19) = 0.39$
10	0.885	0.013	−0.005	0.826	0.016	−0.010	$p(88, 64) = 0.28$
20	0.858	0.012	−0.007	0.791	0.015	−0.010	$p(38, 31) = 0.33$
30	0.908	0.009	−0.005	0.886	0.010	−0.007	$p(17, 12) = 0.58$
				Site B			
5	0.819	0.021	0.004	0.852	0.019	0.000	$p(27, 31) = 0.78$
10	0.862	0.019	−0.002	0.870	0.019	−0.007	$p(19, 31) = 0.92$
20	0.827	0.020	−0.001	0.837	0.019	−0.005	$p(11, 12) = 0.96$
30	0.803	0.025	0.004	0.873	0.020	0.003	$p(12, 11) = 0.75$
				Site C			
5	0.258	0.052	0.045	0.593	0.038	0.017	$p(29, 20) = 0.50$
10	0.542	0.042	0.029	0.656	0.037	0.002	$p(17, 30) = 0.71$
20	0.692	0.029	0.022	0.756	0.025	−0.005	$p(9, 10) = 0.87$
30	0.739	0.023	0.008	0.462	0.033	−0.019	$p(9, 3) = 0.59$

† Probability of Type I Error for hypothesis that RMSD for simulation the using parameters obtained from pressure plate analysis is significantly different from the RMSD using parameters obtained from SFC; numbers in parentheses are the effective sample sizes.

due to water migration to the freezing front, while simulated liquid water content continued to decrease. As the frost front advanced, the 5-cm total water content began to level off, and the 10-cm total water content increased upon freezing on Day 345. Subsequently, the 20-cm depth began to freeze on Day 347. Due to the low unsaturated conductivity of the coarsely textured sites, there was much less moisture migration to the freezing front than for the silt loam Site C. As a result, increase in total water content was much smaller for Sites A and B (as shown for Site B in Fig. 3).

Although RMSDs for the nonfreezing period were not much different and actually improved for some depths compared with the freezing period, ME decreased considerably. This was largely due to the fact that water content varied relatively little through the nonfreezing period without any vegetation to extract water. Indeed, water potential at all three Orchard sites remained above $-500\ J\ kg^{-1}$ for most of the nonfreezing period. Because ME is the fraction of variation in measured values explained by the model, similar errors result in lower ME when observed variation is small.

Influence of Ice Content on TDR readings

Neglecting the effect of ice on TDR-measured liquid water content results in higher estimated water content. This bias tends to be greater at lower liquid water contents and to increase with total water content (i.e., when ice contents are high). The maximum correction for Site C, which had higher total water than the other sites, was 0.010 $m^3\ m^{-3}$ at a corrected water content of 0.045 $m^3\ m^{-3}$. Maximum corrections for Sites A and B (0.006 and 0.007 $m^3\ m^{-3}$) were lower than Site C because of lower initial water content and less ice formation. However, the impact on the estimated SMC parameters was greatest for Site B, in part because it experienced the lowest water contents. A correction of

Table 4. Model performance for simulated daily liquid water content at the Orchard sites during the nonfreezing period (March–June) using parameters based on pressure plate analysis and estimated from the soil freezing characteristic (SFC).

	Pressure plate parameters			SFC parameters			
Depth	ME	RMSD	MBE	ME	RMSD	MBE	*F* test†
cm		$m^3\ m^{-3}$			$m^3\ m^{-3}$		
				Site A			
5	−0.170	0.022	−0.020	−0.982	0.029	−0.027	$p(13, 13) = 0.67$
10	0.653	0.010	−0.004	0.314	0.014	−0.011	$p(59, 16) = 0.35$
20	0.437	0.011	−0.005	−0.122	0.015	−0.013	$p(43, 8) = 0.45$
30	−0.209	0.012	−0.007	−1.338	0.016	−0.014	$p(29, 6) = 0.52$
				Site B			
5	0.392	0.032	0.012	0.366	0.033	0.017	$p(6, 5) = 0.90$
10	0.415	0.030	−0.004	0.516	0.027	0.002	$p(20, 17) = 0.63$
20	−0.195	0.034	−0.016	0.053	0.031	−0.012	$p(8, 8) = 0.55$
30	−0.181	0.034	−0.014	0.046	0.031	−0.012	$p(5, 5) = 0.58$
				Site C			
5	0.029	0.020	0.010	−1.295	0.030	−0.026	$p(27, 6) = 0.38$
10	0.006	0.021	−0.017	−5.830	0.056	−0.054	$p(10, 14) = 0.15$
20	−0.281	0.022	−0.021	−8.060	0.060	−0.059	$p(8, 12) = 0.20$
30	−8.473	0.046	−0.045	−30.87	0.084	−0.084	$p(6, 8) = 0.48$

† Probability of Type I Error for hypothesis that RMSD for the simulation using parameters obtained from pressure plate analysis is significantly different from the RMSD using parameters obtained from SFC; numbers in parentheses are the effective sample sizes.

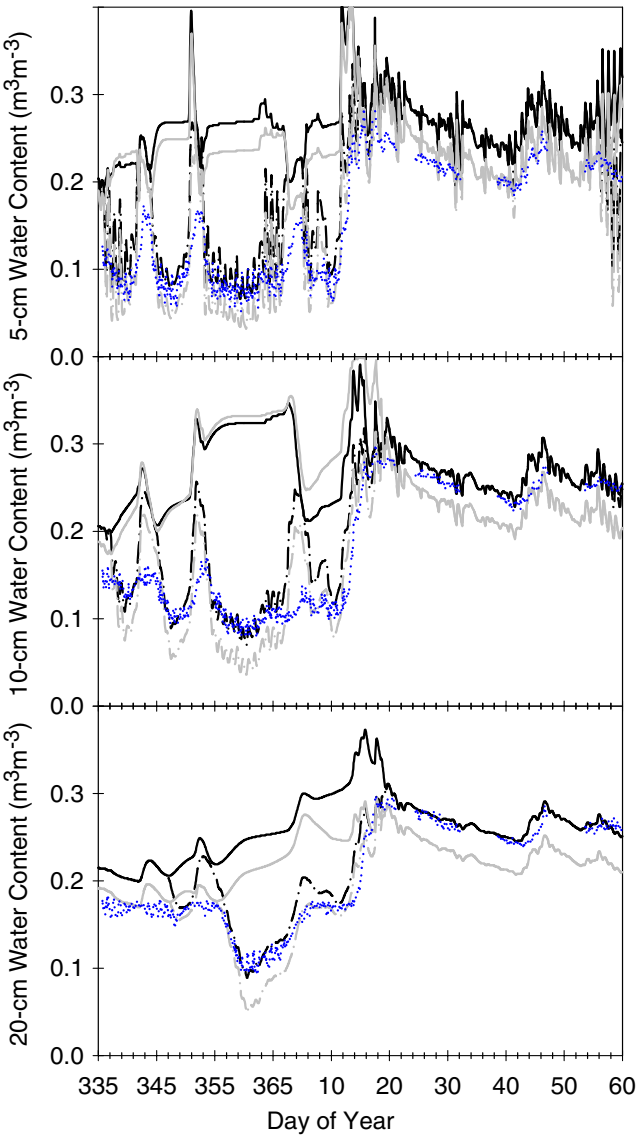

Fig. 4. Simulated hourly water contents using soil moisture characteristic (SMC) parameters estimated from the soil freezing characteristic (SFC) and from pressure plate analyses. Plotted are total water content and simulated and measured liquid water content for the silt loam Orchard Field Site C for the 5-, 10-, and 20-cm depths. (Legend is same as in Fig. 3.)

0.007 m^3 m^{-3} at a water content of 0.016 m^3 m^{-3} is relatively much greater than that experienced at either Site A or C. A small change near zero can have a significant change on a log-log plot and the resulting best-fit line (Fig. 2). Air entry and *b* value for Site B neglecting the effects of ice content were −0.61 J kg^{-1} and 3.15, which are both outside the 90% confidence interval for the parameters obtained with the ice content correction. Simulated liquid water contents using these parameters averaged 0.03 m^3 m^{-3} higher during the nonfreezing period for Site B, whereas they were only 0.01 m^3 m^{-3} higher for Sites A and C using the parameters neglecting the effects of ice content. RMSD using the ice-neglected parameters increased by as much as 0.008 m^3 m^{-3} for the Site B at the 5-cm depth during the freezing period and 0.022 m^3 m^{-3} during the nonfreezing period. RMSD for Sites A and C actually decreased by 0.01 m^3 m^{-3} using the ice-neglected parameters.

Influence of Neglecting Solutes

The SMC parameters were estimated from the SFC while neglecting the effects of osmotic potential in Eq. [2] and [4] to assess its influence on model simulations. In doing so, the resulting *b* values for Sites A, B, and C were 2.67, 2.33, and 2.31, respectively, and computed air entry potentials were −3.4, −3.8, and −15.3 J kg^{-1}. In general, neglecting the effects of solutes introduces a bias toward lower water potentials and shifts the SMC slightly toward more negative potentials. Simulated liquid water contents using these parameters averaged 0.008 m^3 m^{-3} lower for the freezing period and 0.019 m^3 m^{-3} lower for the nonfreezing period compared with using the SFC-based parameters in Table 2. In almost all cases, the RMSD increased using parameters from the SFC neglecting solutes compared with including the effects of solutes. The increase in RMSD ranged from 0.003 m^3 m^{-3} for the Site C freezing period to 0.016 m^3 m^{-3} for Sites A and C during the nonfreezing period.

Application to Rangeland Field Sites

Lower Sheep

Saturated paste extracts were not available for the Lower Sheep site, so the SFCs were analyzed neglecting the effects of solutes. Because TDR measurements were not made for the near-surface depth, the near-surface fiberglass sensors were not individually calibrated and instead a "composite" calibration was used (Seyfried, 1993). The SFC analysis for the near-surface sensors is therefore not presented.

The SFC for the 10-cm depth for the Lower Sheep site plotted in Fig. 5 illustrates the problems that may occur if the soil is too dry for the soil water to freeze. Lack of fall precipitation for several of the years during the study caused the soil to enter the freezing period very dry. Data points to the left of the 1993–1994 data (Fig. 5) represent periods when the soil was too dry to freeze at the temperatures experienced, and the data were useless for establishing the SFC. The fall of 1993–1994, however, had sufficient precipitation to wet the soil and was used for the SFC analysis. The resulting best-fit SMC

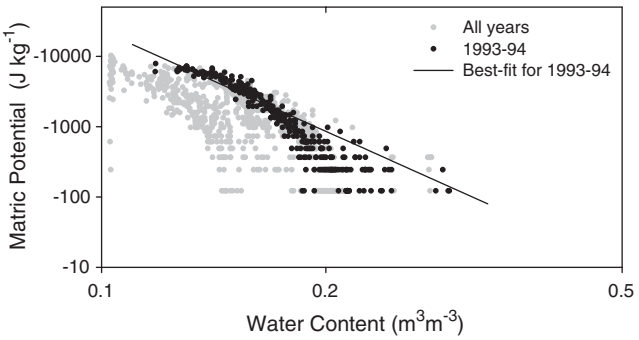

Fig. 5. Log-log plot of matric potential versus water content from in situ measurement of the soil freezing characteristic (SFC) at the Lower Sheep site for the 10-cm depth.

parameters given in Table 2 yielded a coefficient of determination (R^2) of 0.89.

The SHAW model was run for the Lower Sheep site using the best-fit SMC parameters for the respective depths. Saturated hydraulic conductivity was estimated from the SHAW user interface using the algorithm presented by Saxton et al. (1986). Soil temperature and water content were simulated for the bare interspace site through February of 1993 and through March of 1994 starting with the measured 1-m profile on 1 October of the previous year. Measured soil temperature and water at 1 m were used as boundary conditions. Simulated soil water dynamics using the SFC-based parameters agreed well with measured liquid water content for all years simulated, as shown for years 1993–1994 and 1994–1995 in Table 5. The RMSD ranges from 0.018 to 0.035 $m^3\ m^{-3}$, and the bias error is almost negligible in most cases. Simulated water dynamics for 1994–1995 are plotted in Fig. 6. The good agreement between measured and simulated water contents for this year suggests that the SFC can successfully be used across years.

Boise Front

The SFC obtained during the winter of 1999–2000 for Pits 1 and 2 of the Boise Front are plotted in Fig. 7. Pit 1 displays considerable scatter, likely due to the fact that the temperature and moisture sensors were sensing slightly different microenvironments. However, data from Pit 2 follow two distinct curves that represent two distinct freeze–thaw cycles during the winter of 1999–2000. This suggests hysteresis of the SFC and/or the SMC similar to that observed by Spaans and Baker (1996). Best-fit parameters for pore-size distribution, b, and air entry potential, ψ_e, in Eq. [3] are given in Table 2 and yielded a coefficient of determination (R^2) of 0.45.

The SHAW model was run for the Boise Front using the best-fit SMC parameters obtained from the SFC for Pit 2. Saturated hydraulic conductivity was estimated from the SHAW user interface using the algorithm presented by Saxton et al. (1986). Soil temperature and water content were simulated for one entire year starting with the measured 1-m profile on 1 Oct. 1999. Simulations were conducted to a depth of 4 m where soil temperature was assumed constant and water flux was assumed to be by gravity flow only.

Model performance for the Boise Front is summarized in Table 6, showing that the simulation results actually improved for the summer period. Simulated and measured water content for the spring and summer periods are plotted in Fig. 8. The model tracks the dry-

Table 5. Model performance for simulated daily liquid water content during the freezing period (November–February) for the Lower Sheep site.

Depth	ME	RMSD	MBE
cm		$m^3\ m^{-3}$	
	1993–1994		
Near-surface	0.612	0.026	0.004
10	0.754	0.022	−0.004
20	0.864	0.018	0.013
	1994–1995		
Near-surface	0.578	0.021	−0.004
10	0.426	0.035	−0.003
20	0.772	0.030	0.003

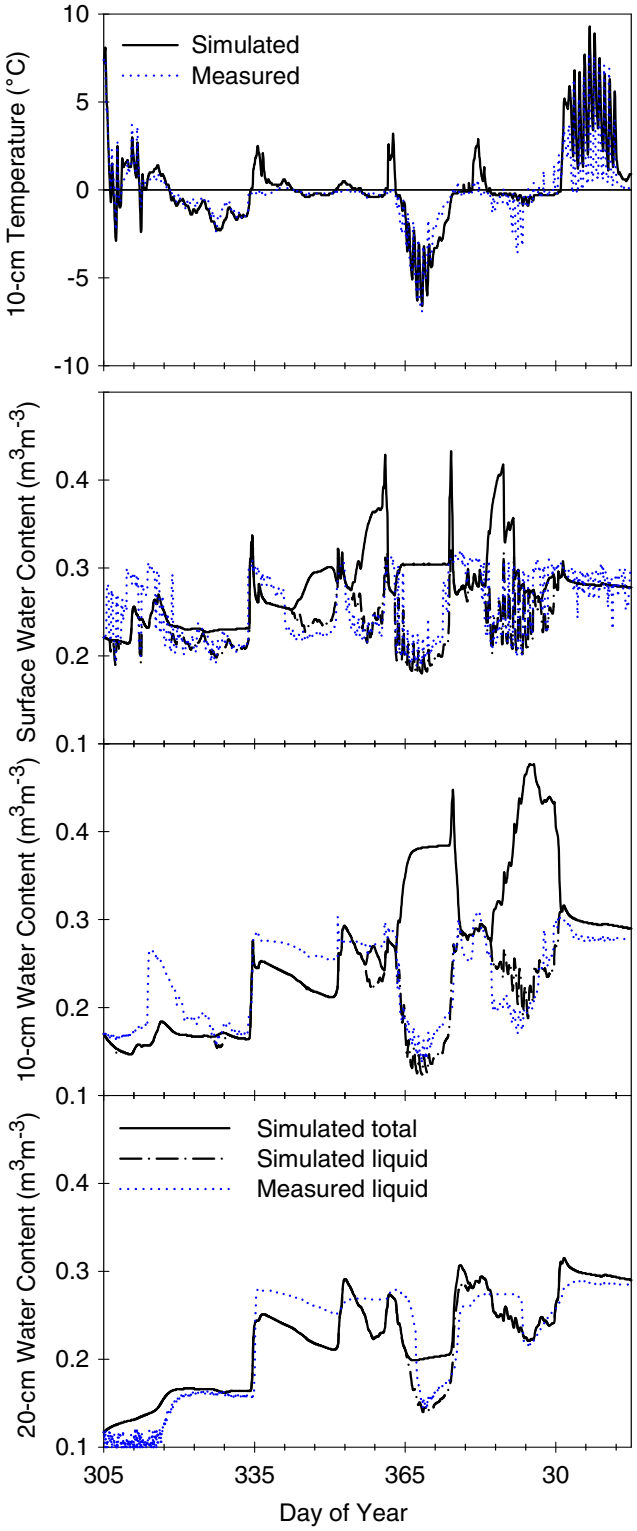

Fig. 6. Simulated total water content and simulated and measured hourly liquid water content for the Lower Sheep site for the near-surface, 10-, and 20-cm depths during the freezing period. Measured and simulated 10-cm soil temperatures are plotted for reference to freeze–thaw cycles.

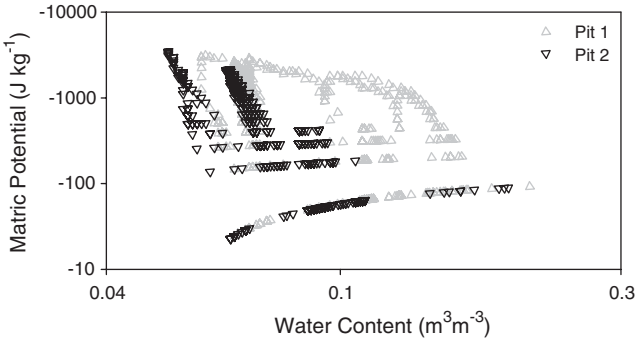

Fig. 7. Log-log plot of matric potential versus water content from in situ measurement of the soil freezing characteristic (SFC) at Pits 1 and 2 of the Boise Front site.

down of the soil moisture through the growing season quite well. Unlike the Orchard site, ME for the Boise Front summer period is higher than that for the winter period (Tables 3, 4, and 6). RMSD ranged from 0.035 to 0.066 $m^3\ m^{-3}$ during the freezing period and from 0.018 to 0.044 $m^3\ m^{-3}$ for the nonfreezing period. Model performance for the 15-cm water content was somewhat poorer than for the other depths for both the freezing and nonfreezing periods. This was due in part to the 15-cm soil water sensor consistently measuring higher during wetter periods. For example, between Days 50 and 90, the 5- and 30-cm sensors hovered around 0.20 $m^3\ m^{-3}$ while the 15-cm sensor read around 0.25 $m^3\ m^{-3}$. This anomaly is likely a result of a local variation in soil structure around this sensor and did not affect drier periods.

By the end of the summer, soil water content dropped as low as 0.03 $m^3\ m^{-3}$ at the 5- and 15-cm depths. This corresponds to a water potential of approximately −10 000 J kg^{-1}. Clearly these soils were dried to this level primarily by evaporation. However, even the 30-cm depth dried to 0.045 $m^3\ m^{-3}$, or −3000 J kg^{-1}. Such water potentials are not out of the realm of transpiration by semiarid plants. Without a reasonable SMC to represent the soil water dynamics in this dry region, it would be difficult to accurately simulate the dry-down to these water contents. Simulation results indicate that the SMC obtained from freezing conditions is applicable to nonfreezing conditions.

DISCUSSION

A few issues limit the usefulness of in situ SFC as a surrogate for the SMC. An obvious limitation is the necessity for freezing temperatures, but the soil must also

Table 6. Model performance for simulated daily liquid water content during the freezing (October–February) and nonfreezing (February–September) periods for Boise Front.

Depth	ME	RMSD	MBE
cm		$m^3\ m^{-3}$	
	Freezing		
5	0.755	0.035	−0.027
15	0.461	0.066	−0.048
30	0.685	0.039	−0.023
	Nonfreezing		
5	0.949	0.018	−0.011
15	0.710	0.044	−0.037
30	0.808	0.028	−0.025

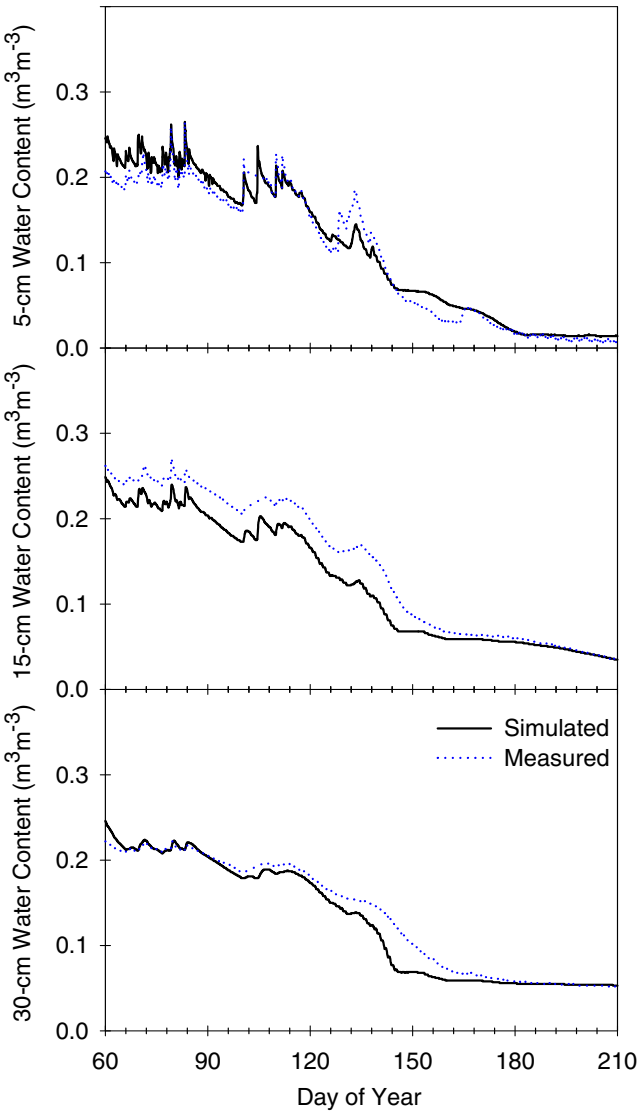

Fig. 8. Simulated and measured hourly liquid water content for the Boise Front site for the 5-, 15-, and 30-cm depths during the nonfreezing period.

be sufficiently wet for the soil water to freeze at the subzero temperatures (°C) experienced. If the soil is sufficiently dry such that the soil water potential is below the equilibrium water potential given by Eq. [2], soil water will not freeze. Without ice present, the relation between temperature and soil water potential does not apply, as was demonstrated for the Lower Sheep site.

A second complication is the influence of ice on liquid water content measurements obtained from TDR-based methods. Because the permittivity of ice is greater than that of air, elevated ice content will result in an overestimation of liquid water content, introducing a bias in the SMC. The bias is most severe at very low water potentials when much of the total water content is ice. An approximate correction for ice content was used herein. Accurate correction for ice content requires knowledge of total water content, which can be problematic for in situ applications because the sample volume of methods to measure total water content, such as

neutron probe, is much different than that of TDR. Spaans and Baker (1995) reported errors in TDR measurements as high as 0.02 $m^3\ m^{-3}$ at very high ice contents. The maximum correction observed in our study was 0.01 $m^3\ m^{-3}$. While this correction may be quite small, it can have a significant effect on the computed SMC when it is applied to very low water contents, as observed for Orchard Site B. Uncorrected readings from calibrated fiberglass resistance sensors at the Lower Sheep site seemed to work well for developing the SFC.

As pointed out by Spaans and Baker (1996), the SFC may have limitations at high liquid water contents. The osmotic potential becomes a relatively larger component of the total water potential when the soil is relatively wet. For the soils tested herein, osmotic potential ranged from approximately -3 J kg^{-1} near saturation to $<1\%$ of the total potential for extremely dry conditions ($-10\,000$ J kg^{-1}). Additionally, small uncertainties in the temperature measurement become very critical near saturation as much of the water freezes over a small temperature range. Each 0.1°C increment corresponds to approximately 120 J kg^{-1}. More accurate temperature measurements may be possible, but are typically not used in field installations. Small differences in the sampling environment between the temperature and water sensors can exacerbate this sensitivity to soil temperature, as suggested for the Boise Front Pit 1. These errors can be relatively large at high water potentials, but become minimal at low water potentials.

CONCLUSIONS

The utility of deriving the SMC in situ from measurements of soil temperature and liquid water content during freezing periods based on its relation to the SFC was explored. Soil moisture characteristic curves obtained by pressure plate analysis were compared with the in situ soil freezing characteristic obtained for three different soil types at the Orchard Field Site in southwestern Idaho. The curves agreed well for the loamy sand soil, but the SFC showed a slight bias toward higher water potentials for the sandy loam and silt loam soils compared with the pressure plate measurements. Frozen and unfrozen soil water dynamics simulated by the SHAW model using the SMC derived from the SFC agreed well with measured soil water contents. Compared with simulations using SMC parameters based on pressure plate analysis, the RMSD changed by -0.014 to $+0.010$ $m^3\ m^{-3}$ during the freezing period and by -0.007 to $+0.038\ m^3\ m^{-3}$ during the nonfreezing period. Complications arising from solute effects and the influence of ice content on TDR readings were investigated and shown to be minor in most cases, and limitation of the SFC at high water contents was discussed. However, derivation of the SMC from the SFC can be a very useful tool, particularly for arid and semiarid areas where soils can reach potentials of $-10\,000$ J kg^{-1}.

ACKNOWLEDGMENTS

Data collection at the Boise Front site was supported by a grant from NASA (Grant number NAG5-7537).

REFERENCES

Bittelli, M., M. Flury, and G.S. Campbell. 2003. A thermodielectric analyzer to measure the freezing and moisture characteristic of porous media. Water Resour. Res. 39(2):1041. doi:10.1029/2001WR000930.

Bittelli, M., M. Flury, and K. Roth. 2004. Use of dielectric spectroscopy to estimate ice content in frozen porous media. Water Resour. Res. 40(4):W04212. doi:10.1029/2003WR002343.

Campbell, G.S. 1974. A simple method for determining unsaturated conductivity from moisture retention data. Soil Sci. 117:311–314.

Campbell Scientific. 1996. Instruction manual. CS615 Water Content Reflectometer. Campbell Scientific, Logan, UT.

Campbell, G.S., and R.Y. Anderson. 1998. Evaluation of simple transmission line oscillators for soil moisture measurement. Comput. Electron. Agric. 20:31–44.

Chandler, D.G., M. Seyfried, M. Murdock, and J.P. McNamara. 2004. Field calibration of water content reflectometers. Soil Sci. Soc. Am. J. 68:1501–1507.

Celia, M.A., E.T. Bouloutas, and R.L. Zarba. 1990. A general mass-conservative numerical solution for the unsaturated flow equation. Water Resour. Res. 26:1483–1496.

Flerchinger, G.N., J.M. Baker, and E.J.A. Spaans. 1996a. A test of the radiative energy balance of the SHAW model for snowcover. Hydrol. Processes 10:1359–1367.

Flerchinger, G.N., K.R. Cooley, and Y. Deng. 1994. Impacts of spatially and temporally varying snowmelt on subsurface flow in a mountainous watershed: 1. Snowmelt simulation. Hydrol. Sci. J. 39: 507–520.

Flerchinger, G.N., C.L. Hanson, and J.R. Wight. 1996b. Modeling evapotranspiration and surface energy budgets across a watershed. Water Resour. Res. 32:2539–2548.

Flerchinger, G.N., and S.P. Hardegree. 2004. Modelling near-surface temperature and moisture of post-wildfire seedbed for germination response predictions. J. Arid Environ. 59:369–385.

Flerchinger, G.N., W.P. Kustas, and M.A. Weltz. 1998. Simulating surface energy fluxes and radiometric surface temperatures for two arid vegetation communities using the SHAW model. J. Appl. Meteorol. 37:449–460.

Flerchinger, G.N., and F.B. Pierson. 1991. Modeling plant canopy effects on variability of soil temperature and water. Agric. For. Meteorol. 56(3–4):227–246.

Flerchinger, G.N., and K.E. Saxton. 1989. Simultaneous heat and water model of a freezing snow-residue-soil system I. Theory and development. Trans. ASAE 32:565–571.

Fuchs, M., G.S. Campbell, and R.I. Papendick. 1978. An analysis of sensible and latent heat flow in a partially frozen unsaturated soil. Soil Sci. Soc. Am. J. 42:379–385.

Gee, G.W., and J.W. Bauder. 1986. Particle-size analysis. p. 383–411. *In* A.L. Page et al. (ed.) Methods of soil analysis. Part 1. 2nd ed. Agron. Monogr. 9. ASA and SSSA, Madison, WI.

Hayhoe, H.N. 1994. Field testing of simulated soil freezing and thawing by the SHAW model. Can. Agric. Eng. 36:279–285.

Hymer, D.C., M.S. Moran, and T.O. Keefer. 2000. Soil water evaluation using a hydrologic model and calibrated sensor network. Soil Sci. Soc. Am. J. 64:319–326.

Kelleners, T.J., M.S. Seyfried, J.M. Blonquist, Jr., J. Bilskie, and D.G. Chandler. 2005. Improved interpretation of water content reflectometer measurements in soils. Soil Sci. Soc. Am. J. 69: 1684–1690.

Kennedy, I., and B. Sharratt. 1998. Model comparisons to simulate frost depth. Soil Sci. 163:636–645.

Koopmans, R.W.R., and R.D. Miller. 1966. Soil freezing and soil water characteristics curves. Soil Sci. Soc. Am. Proc. 30:680–685.

Lee, J., and R. Lund. 2004. Revisiting simple linear regression with autocorrelation errors. Biometrika 91:240–245.

McDonald, E.V. 2002. Numerical simulations of soil water balance in support of revegetation of damaged military lands in arid regions. Arid Land Res. Manage. 16:277–290.

Parkin, G.W., C. Wagner-Riddle, D.J. Fallow, and D.M. Brown. 1999. Estimated seasonal and annual water surplus in Ontario. Can. Water Resour. J. 24:277–292.

Rhoades, J.D. 1986. Soluble salts. p. 167–179. *In* A.L. Page et al. (ed.) Methods of soil analysis. Part 2. 2nd ed. Agron. Monogr. 9. ASA and SSSA, Madison, WI.

Saxton, K.E., W.J. Rawls, J.S. Romberger, and R.I. Papendick. 1986. Estimating generalized soil water characteristics from texture. Soil Sci. Soc. Am. J. 50:1031–1036.

Seyfried, M.S. 1993. Field calibration and monitoring of soil-water content with fiberglass electrical resistance sensors. Soil Sci. Soc. Am. J. 57:1432–1436.

Seyfried, M.S., and M.D. Murdock. 1996. Calibration of time domain reflectometry for measurement of liquid water content in frozen soils. Soil Sci. 161:87–98.

Seyfried, M.S., and M.D. Murdock. 2001. Response of a new soil water sensor to variable soil, water content, and temperature. Soil Sci. Soc. Am. J. 65:28–34.

Seyfried, M.S., S. Schwinning, M.A. Walvoord, W.T. Pockman, B.D. Newman, R.B. Jackson, and F.M. Phillips. 2005. Ecohydrological control of deep drainage in arid and semiarid regions. Ecology 86: 277–287.

Soilmoisture. 1990. Trase, System 1. Operating instructions. Soilmoisture Equipment Corp., Santa Barbara, CA.

Spaans, E.J.A., and J.M. Baker. 1995. Examining the use of time domain reflectometry for measuring liquid water content in frozen soil. Water Resour. Res. 31:2917–2925.

Spaans, E.J.A., and J.M. Baker. 1996. The soil freezing characteristic: Its measurement and similarity to the soil moisture characteristic. Soil Sci. Soc. Am. J. 60:13–19.

Topp, G.C., J.L. Davis, and A.P. Annan. 1980. Electromagnetic determination of soil water content: Measurement in coaxial transmission lines. Water Resources Research 16:574–582.

Xu, X., J.L. Nieber, J.M. Baker, and D.E. Newcomb. 1991. Field testing of a model for water flow and heat transport in variably saturated, variably frozen soil. p. 300–308 *In* Transportation Research Record 1307. Transportation Research Board, National Research Council, Washington, DC.